JACS
JOURNAL OF THE AMERICAN CHEMICAL SOCIETY

Article

pubs.acs.org/JACS

Helicity as a Steric Force: Stabilization and Helicity-Dependent Reversion of Colored *o*-Quinonoid Intermediates of Helical Chromenes

Jarugu Narasimha Moorthy,* Susovan Mandal, Arindam Mukhopadhyay, and Subhas Samanta

Department of Chemistry, Indian Institute of Technology, Kanpur 208016, India

Supporting Information

ABSTRACT: Photolysis of regioisomeric helical chromenes **1** and **2** leads to colored reactive intermediates. While the latter generally decay quite rapidly, they are found to be longer lived in **1** and highly persistent in **2**. The remarkable stability of the otherwise fleeting transient in **2** allowed isolation and structural characterization by X-ray crystallography. The structural analyses revealed that steric force inherent to the helical scaffold is the origin of stability as well as differentiation in the persistence of the intermediates of **1** and **2** (**1Q** and **2Q**). The structure further shows that diphenylvinyl moiety in the TT isomer of **2Q** gets splayed over the helical scaffold such that it is fraught with a huge steric strain to undergo required bond rotations to regenerate the precursor chromene. Otherwise, reversion of **2Q** was found to occur at higher temperatures. Aazahelical chromenes **3** and **4** with varying magnitudes of helicity were designed in pursuit of *o*-quinonoid intermediates with graded activation barriers. Their photogenerated intermediates **3Q** and **4Q** were also isolated and structurally characterized. The activation barriers for thermal reversion of **2Q**–**4Q**, as determined from Arrhenius and Eyring plots, are found to correlate nicely with the helical turn, which decisively determines the steric force. The exploitation of helicity is thus demonstrated to develop a novel set of photoresponsive helicenes **2**–**4** that lead to colored intermediates exhibiting graded stability. It is further shown that the photochromism of **2**–**4** in conjunction with response of **2Q**–**4Q** to external stimuli (acid, heat, and visible radiation) permits development of molecular logic gates with INHIBIT function.

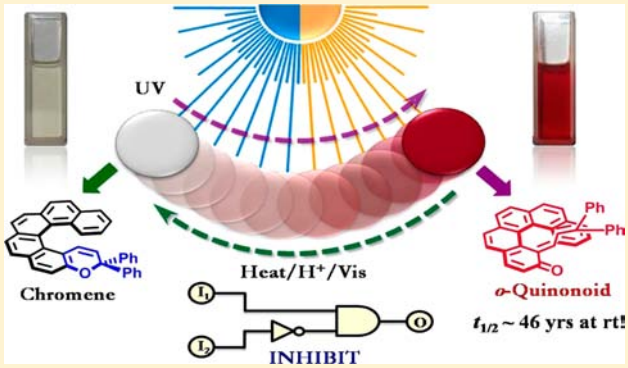

INTRODUCTION

Helicity is ubiquitous in all forms that besiege our day-to-day life.[1,2] Aside from the fact that it constitutes the structure of a basic unit of life, namely DNA, and gigantic galaxies that are inherent in the composition of the universe, helicity appears to be indispensable in the nature's wiliest designs and creations—be it in a plant/animal kingdom or in a materialistic world.[3−5] For chemists, helical structures have traditionally represented aesthetic marvels. The initial and pioneering work of Newman on helical organic structures spawned a great deal of interest in the properties of helicenes.[6,7] Over the past decade or so, there has been a swarming interest in exploring the utility of helicity in a variety of applications. Today, the helical scaffold essentially forms a design element in the development of recognition-based sensors,[8,9] molecular switches,[10] springs,[11] motors,[12] tweezers,[13] solenoids,[14] organic electronics,[15] IR-sensing[16] and display devices,[17] NLO materials and thin films,[18] liquid crystalline materials,[19] polymers,[20] etc. As applied to biology, helicenes, by virtue of their inherent chirality, are obvious choices for efficient chiral selection in DNA binding and intercalation, telomerase inhibition, etc.[21,22] The remarkably higher optical rotations confer helicenes with unique opportunities for exploration in the development of chiroptical materials.[23,24] Insofar as molecular recognition is concerned, there has been remarkable progress in harvesting exceptional enantiodifferentiating potential of helicenes for creation of organocatalysts; diverse catalysts based on helicenes with ingenious designs continue to be explored in pursuit of high enantioselectivity in asymmetric synthesis.[25,26] Helicenes or helicenoids[27,28] elicit tremendous excitement in the context of photoresponsive materials.

2,2-Diarylbenzopyrans, termed generally chromenes, are a unique class of photochromic compounds that are industrially useful in ophthalmic lenses.[29−32] Irradiation of chromenes with UV radiation brings about C−O bond cleavage leading to the so-called *o*-quinonoid intermediates that are colored; the latter revert thermally as well as photochemically with visible light. While the photochromic phenomenon of chromenes, spiropyrans, is widely explored in ophthalmic lenses, their application as molecular switches in optical data storage devices is limited by the rapid thermal reversion of the photogenerated colored forms.[33] Thus, modulation of spectrokinetic properties of the photogenerated *o*-quinonoid intermediates and hence the

Received: December 10, 2012
Published: April 10, 2013

Chart 1

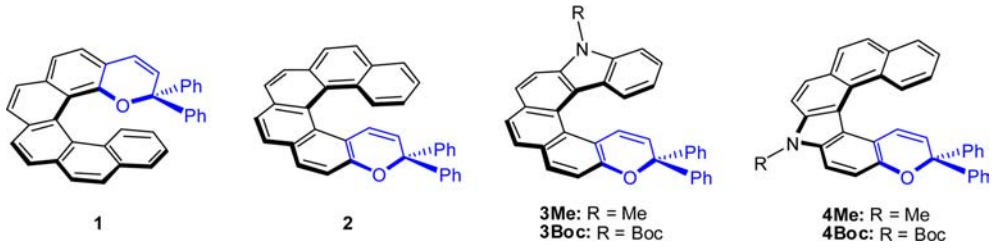

Scheme 1. Synthesis of Helical Chromenes 1−4[a]

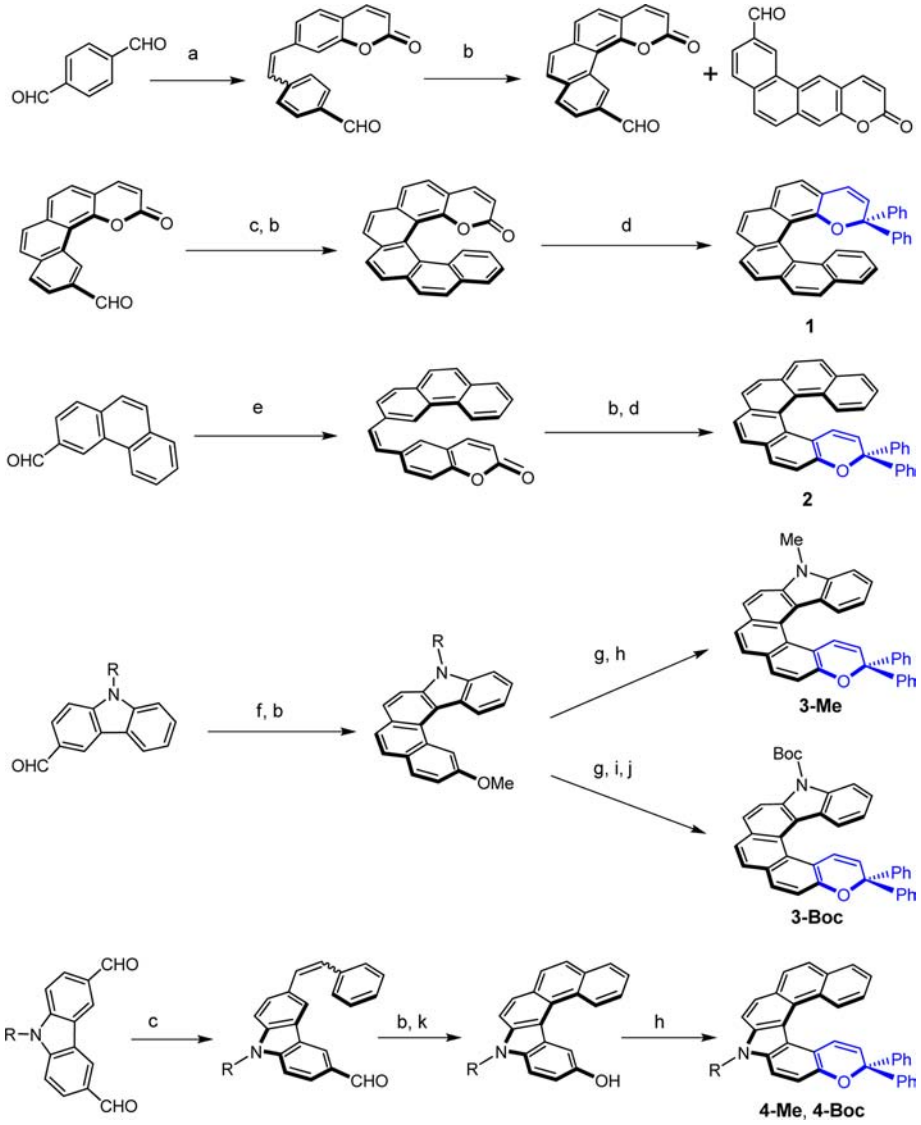

[a](a) (7-Coumaryl)methyltriphenylphosphonium bromide, 50% NaOH, DCM, 0 °C to rt, 3 h; (b) *hν*, I_2, O_2, toluene, 24 h; (c) benzyltriphenylphosphonium bromide, 50% NaOH, DCM, 0 °C to rt, 3 h; (d) (i) PhMgBr/THF, (ii) H^+, rt; (e) (6-coumaryl)-methyltriphenylphosphonium bromide, 50% NaOH, DCM, 0 °C to rt, 3 h; (f) (4-methoxybenzyl)triphenylphosphonium bromide, 50% NaOH, DCM, 0 °C to rt, 3 h; (g) BBr_3, dry DCM, 0 °C to rt, 6 h; (h) 1,1-diphenylpropargyl alcohol, PPTS, dry DCE, reflux, 24 h; (i) $(Boc)_2O$, TEA, DMAP, THF, 0 °C to rt, 12 h; (j) 30% piperidine in DCM, rt, 12 h; (k) H_2O_2, Conc. H_2SO_4, DCM−MeOH, rt, 48 h.

photochromic phenomenon of chromenes has been a subject of extensive investigations.[32,34] Our own interest centers in the phenomenon of photochromism, and we have been interested in the modulation of photochromic property exhibited by chromenes.[35] Buoyed by our preliminary investigations on pentahelical chromenes, which offered a glimpse into the effect of helical scaffold as a steric force on the behavior of colored intermediates,[35a] we designed regioisomeric hexahelical chromenes **1** and **2** (Chart 1) to unambiguously exemplify the role of helicity in modulating the photochromic behavior. The analogous azahelical chromenes **3** and **4** were subsequently designed and synthesized, and their photochromic behavior

dx.doi.org/10.1021/ja312027c | J. Am. Chem. Soc. 2013, 135, 6872−6884

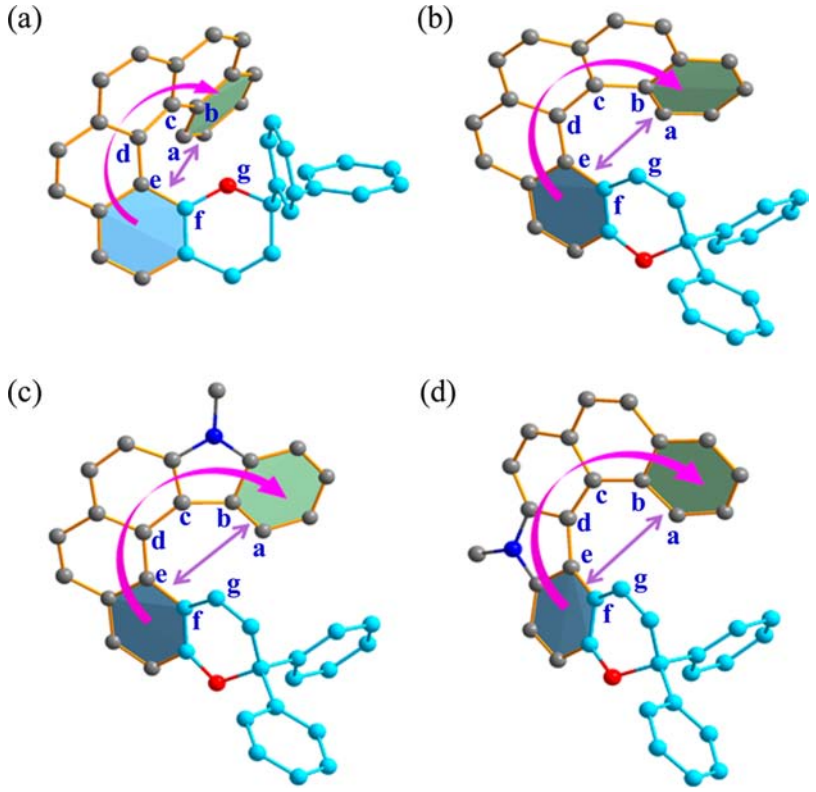

Figure 1. Perspective drawings of the X-ray determined molecular structures of regioisomeric helical chromenes **1** and **2** (a and b), and heterohelical chromenes **3Me** (c) and **4Me** (d).

investigated. Herein, we show that helical scaffold in molecular systems, such as **2**−**4** (Chart 1), can be a unique steric force to stabilize the otherwise fleeting photogenerated colored *o*-quinonoid intermediates to the extent that they can be isolated as solid materials and their structures determined by X-ray crystallography. Reversion of these intermediates to the colorless forms occurs upon heating. We show that the reversion kinetics can be modulated by manipulating the magnitude of steric force, which is determined by the curvature of the helical arc. Subtle variations in the helicities of chromenes **2**−**4** (Chart 1) are shown to manifest differently in the stabilities of their respective *o*-quinonoid intermediates to permit development of thermoresponsive materials that revert at graded temperatures. Indeed, the photochromic phenomena of **2**−**4** in conjunction with the response of their stable colored intermediates to external stimuli, such as acid, heat, and visible radiation, permit development of molecular logic gates with INHIBIT function for application in optical data storage devices.

RESULTS AND DISCUSSION

Synthesis of Helical Chromenes. The regioisomeric carbohelical chromenes **1** and **2** were synthesized from precursor helical coumarins via Grignard reaction followed by dehydration. The helical coumarins were in turn prepared by oxidative photocyclization of the diarylolefins accessed by Wittig olefination, cf. Scheme 1. The azahelical chromenes **3Me** and **3Boc** were prepared by subjecting the suitably functionalized phenols to cyclocondensation with 1,1-diphenylpropargyl alcohol in the presence of pyridinium-*p*-toluenesulfonate (PPTS) as a catalyst in dry 1,2-dichloroethane at reflux. The required hydroxy-substituted helical carbazole derivatives were prepared by a sequence of reactions involving Wittig olefination, oxidative cyclization, and Dakin reaction, cf. Scheme 1. Similarly, chromenes **4Me** and **4Boc** were prepared starting from 3,6-diformylcarbazole by an analogous sequence of reactions mentioned above. The phenols were then transformed to the chromenes by reacting with 1,1-diphenylpropargyl alcohol using PPTS as a catalyst. All the helical chromenes were comprehensively characterized by IR, NMR, and mass spectral data.

X-ray Crystal Structures of Chromenes 1−**4.** We were successful in obtaining the crystals of **1**, **2**, **3Me**, and **4Me** suitable for X-ray analysis, while persistent efforts with crystallization of **3Boc** and **4Boc** were in vain. X-ray diffraction intensity data collection for the crystals of **1**, **2**, **3Me**, and **4Me** was carried out at 100 K on a Smart Apex CCD diffractometer. Subsequently, the structure determinations and refinements were performed using SHELX suit of programs. In Figure 1 are shown the perspective drawings of the molecular structures of these helical chromenes. In all of these structures, one observes considerable deformation of aromatic rings from planarity effected evidently by the helicity. In order to gauge the relative helicities of chromenes **2**−**4**, one may consider a number of parameters, i.e., θ, d, ψ_1, ψ_2, and φ_{total}. The parameter 'd' is the distance between the center of the benzene ring to which the pyran ring is annulated and the center of the terminal benzene ring. Similarly, the parameter 'θ' describes the angle between the mean planes of the two aromatic rings for which the parameter 'd' is calculated. The twist angles ψ_1 and ψ_2 refer to the torsion angles for the atoms a−b−f−g and b−c−e−f, as shown in Figure 1. The sum of torsion angles for the atoms of inner helicene, i.e., a−b−c−d, b−c−d−e, c−d−e−f, and d−e−f−g, is denoted by φ_{total}. The values of d (Å), θ (°), ψ_1 (°), ψ_2

dx.doi.org/10.1021/ja312027c | J. Am. Chem. Soc. 2013, 135, 6872−6884

(°), and φ_{total} (°) calculated for all chromenes **2**–**4** are collected in Table 1 along with those for the regiohelical chromene **1** for comparison. The expectation here is that with increasing helical turn, the terminal benzene ring should become closer to the diphenylpyran moiety such that steric repulsions may cause the terminal benzene ring to twist considerably. Thus, a smaller value for d and a larger value for θ should reflect more helicity. It thus emerges that the helicity for **2**–**4** follows the trend: **2** > **3** > **4**. This trend is completely corroborated by twist angles ψ_1 and ψ_2 as well as the sum of torsion angles φ_{total}.

Table 1. Geometrical Parameters of Chromenes 1, 2, 3Me, and 4Me

parameters	1	2	3Me	4Me
θ (°)	63.99	46.84	45.76	38.06
d (Å)	5.20	5.05	5.49	5.63
ψ_1 (°)[a]	110.15	112.05	91.28	74.73
ψ_2 (°)[b]	52.59	44.48	39.62	26.99
φ_{total} (°)[c]	68.00	77.22	68.75	61.09

[a]The twist angle a–b–f–g. [b]The twist angle b–c–e–f. [c]Sum of torsion angles: a–b–c–d, b–c–d–e, c–d–e–f, and d–e–f–g.

Photochemistry of Regioisomeric Helical Chromenes 1 and 2 and Heterohelical Chromenes 3 and 4. Exposure of the solutions of chromenes **1** and **2** in mesitylene/1,2-dichlorobenzene (5×10^{-3} M) to UV-radiation ($\lambda_{ex} \simeq 350$ nm) under N_2 atmosphere led to instant blood-red coloration. While the color in **1** was found to bleach on standing in the dark within a few minutes, that in the case of **2** was found to be remarkably persistent. In Figure 2 are shown the absorption spectra before and after irradiation, which reveal that the absorptions for **1** and **2** terminate at ~435 nm, while strong absorptions in the visible region extend down to 650 nm for the colored intermediates generated subsequent to photolysis. It is noteworthy that some fine structure is apparent for the absorption spectra of chromenes **1** and **2** in contrast to a broad feature that is observed for the photogenerated colored

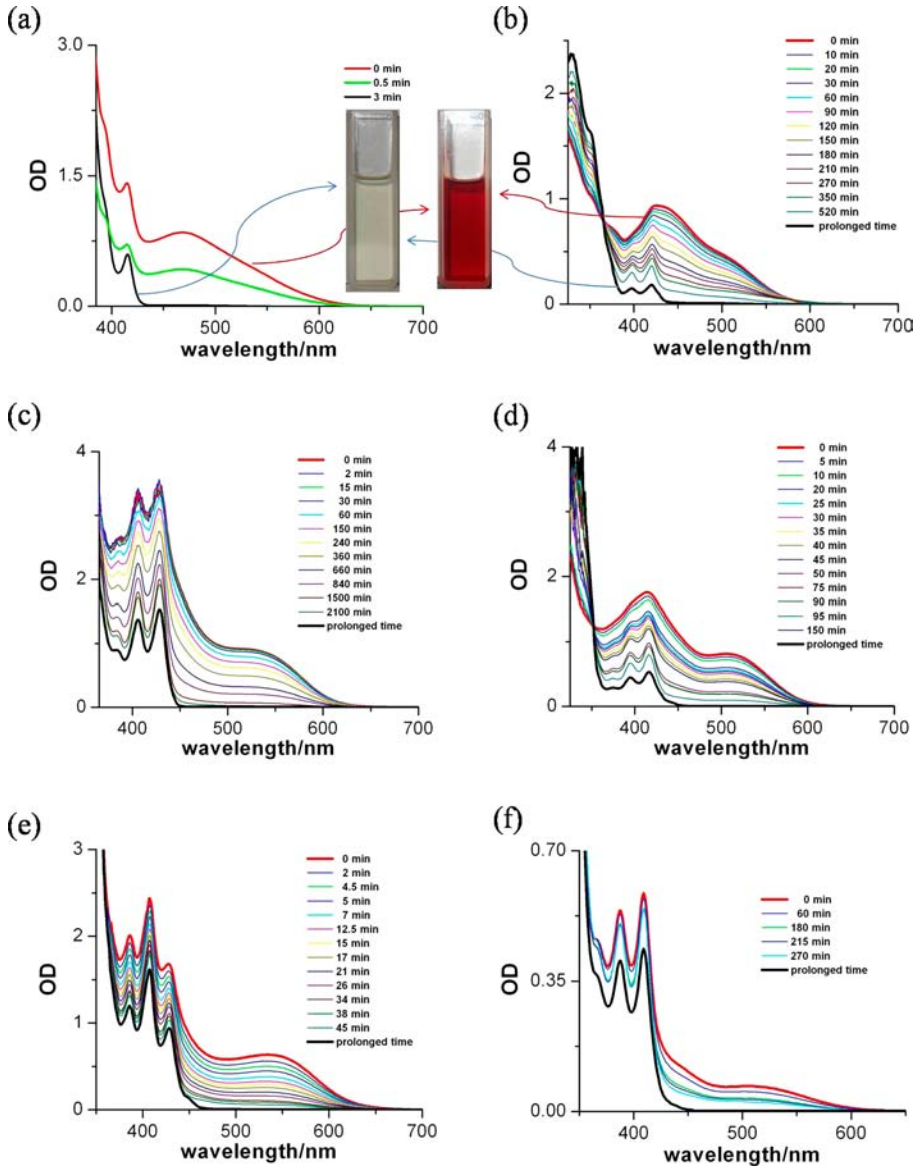

Figure 2. Absorption spectra of chromenes **1** (a), **2** (b), **3Me** (c), **3Boc** (d), **4Me** (e), and **4Boc** (f) before (black) and after irradiation (red). The thermal reversion of the colored species is also shown when monitored at 298 and 373 K for **1** and **2**–**4**, respectively.

dx.doi.org/10.1021/ja312027c | J. Am. Chem. Soc. 2013, 135, 6872–6884

Table 2. Activation Energy (E_a), Pre-Exponential Factor (A), $\Delta H^{\ddagger}$ $\Delta S^{\ddagger}$, Rate Constant for Thermal Bleaching at 353 K, and Half-Life ($t_{1/2}$) at 298 K for Each of the *o*-Quinonoid Intermediates 2Q–4Q

entry	compound	2Q	3MeQ	3BocQ	4MeQ	4BocQ
1	E_a (kcal mol^{-1})	30.52	28.48	28.83	26.80	24.36
2	log A	13.20	12.64	12.83	12.22	10.86
3	$\Delta H^{\ddagger}$ (kcal mol^{-1})	29.70	27.86	28.21	26.11	23.73
4	$\Delta S^{\ddagger}$ (cal K^{-1} mol^{-1})	−1.01	−2.84	−1.97	−4.95	−10.98
5	k (s^{-1})	0.20×10^{-5}	1.20×10^{-5}	0.99×10^{-5}	4.17×10^{-5}	6.23×10^{-5}
6	$t_{1/2}$ at 298 K	46 yrs	4.6 yrs	5.3 yrs	253 d	94 d

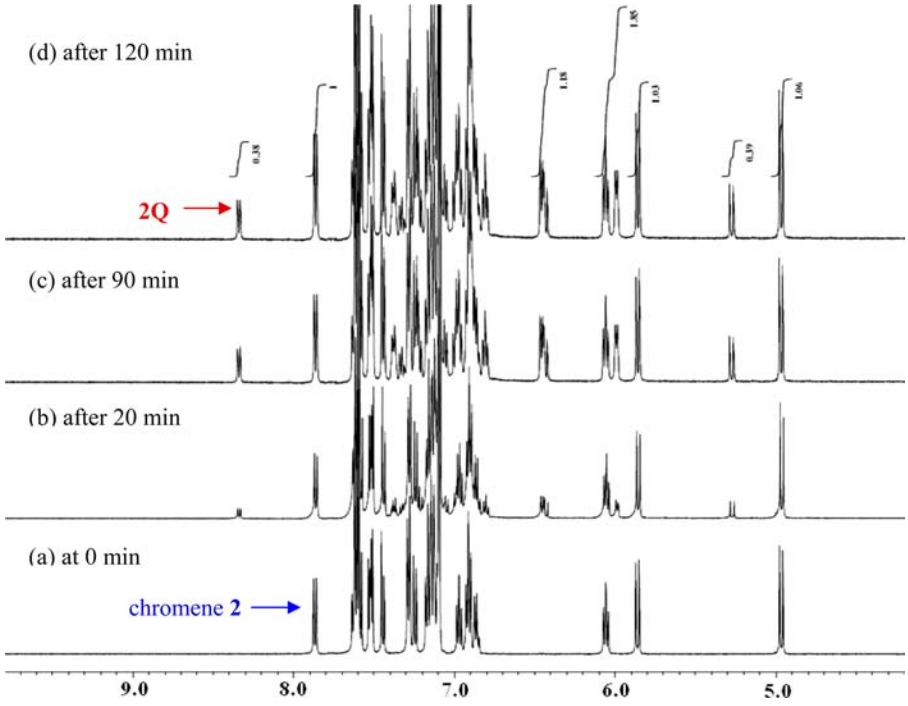

Figure 3. ^{1}H NMR spectra (500 MHz, C_6D_6) of helical chromene **2** and its photolysates with increasing duration of irradiation at 350 nm. Notice the appearance of new signals that is attributable to the formation of a single product, namely, *o*-quinonoid intermediate **2Q**.

Figure 4. X-ray determined molecular structures of the *o*-quinonoid intermediates derived from helical chromenes **2**, **3Boc**, and **4Me**.

intermediates in the visible region. All of the heterohelical chromenes **3** and **4** were found to exhibit photochemical behavior akin to that of chromene **2**. Photolysis of chromenes **3Me** and **3Boc** yielded colored intermediates that are highly persistent. In comparison, the intermediates of **4Me** and **4Boc** were found to be comparatively less stable; the bleaching was found to occur slowly at room temperature over a few days in the case of **4Boc**.

Decay Kinetics of the Colored Intermediates. Given that the photogenerated colored intermediates of chromenes generally revert quite rapidly as observed with helical chromene **1** in the present investigation, remarkable persistence observed for the intermediates of chromenes **2**–**4**, i.e., **2Q**–**4Q**, is intriguing. Bleaching of the color was found to occur upon heating the solutions as monitored by UV–vis absorption spectroscopy, cf. Figure 2. Thus, temperature-dependent decay kinetics of the colored intermediates were carried out over a range of temperatures by following the disappearance of absorption at 524 nm in each case, cf. Supporting Information. From the rate constants thus extracted, Arrhenius free energy of activation (E_a) and the pre-exponential factor (A) were determined for reversion of each of the intermediates, i.e., **2Q**–**4Q**, Table 2. Similarly, the enthalpy and entropy of activation were also determined from Eyring plots, cf. Table 2 and Supporting Information. Accordingly the barriers for reversion of the colored intermediates of **2**–**4** follow the

dx.doi.org/10.1021/ja312027c | J. Am. Chem. Soc. 2013, 135, 6872–6884

order: **2Q** > **3MeQ** ≈ **3BocQ** > **4MeQ** > **4BocQ**. The half-lives ($t_{1/2}$) as determined from Arrhenius equation also follow the same trend, see entry 6.

X-ray Structural Characterization of the Colored Intermediates. ^{1}H NMR monitoring of the photolysates of **2**−**4** revealed the formation of only one colored isomer. In Figure 3 are shown the ^{1}H NMR spectra of the photolysates of chromene **2** with increasing duration of irradiation at 350 nm in a photoreactor. As can be seen, the signals corresponding to the colored intermediate appear distinctly, and their formation saturates with time pointing to attainment of photostationary state (pss) at which the relative concentration of the colored intermediate is 28%. A similar behavior is observed for all other chromenes **3**−**4**, cf. Supporting Information.

The exceptional stabilities of the colored intermediates **2Q**-**4Q** spurred us to isolate them and establish their structures by X-ray crystallography. From a comprehensive analytical data, the products of all chromenes **2**−**4** were identified as *o*-quinonoid intermediates. Crystallization of the colored photoproducts by slow evaporation led to the crystals of **2Q**, **3BocQ**, and **4MeQ** suitable for X-ray studies. The perspective drawings of the molecular structures are shown in Figure 4. Clearly, they correspond to the *o*-quinonoid intermediates formed subsequent to C−O bond cleavage. What is noteworthy is that the geometry of the *o*-quinonoid intermediate in each case corresponds to TT configuration, vide infra.

Activation Barriers for Racemization of *o*-Quinonoid Intermediates. To address the question as to whether thermal decomposition of the colored intermediates is competed by racemization, the enantiomers of a representative quinonoid intermediate, namely **3BocQ**, were resolved with an AD-H chiral column using HPLC. Thus, thermal decomposition of one of the optically pure enantiomer (let us say 'A', Scheme 2)

Scheme 2. Reversion and Concomitant Inversion/Racemization of a Representative *o*-Quinonoid Intermediate 3BocQ with Heating

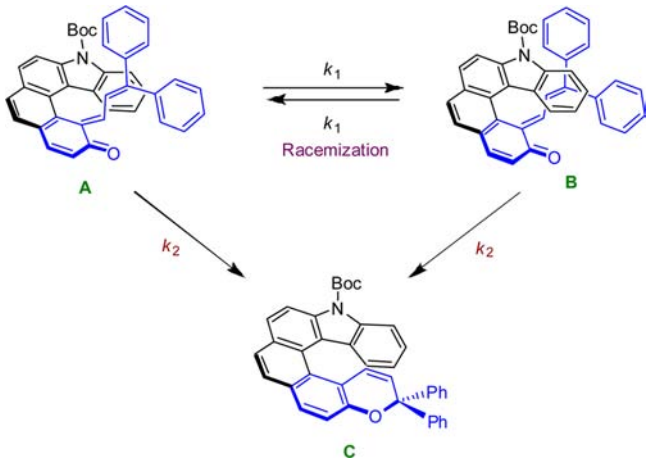

was followed at different intervals of time using HPLC. As the chiral isomer 'A' depleted with time on heating, the amounts of formation of its enantiomer 'B' and the reversion product, i.e., chromene, 'C', were determined by analyzing the reaction mixture with a chiral HPLC. Based on the areas of the starting chiral **3BocQ** (A), its enantiomer (B), and thermally regenerated chromene (C), the rate of inversion/racemization, i.e., A → B, was determined based on the rate equation developed for the Scheme 2, cf. Supporting Information.

The integrated rate law for the Scheme 2 is given by:

$$\frac{[A]_t}{[A]_0} = \frac{1}{2}\left[e^{-k_2 t} + e^{-(2k_1+k_2)t}\right]$$

Based on the above expression, the rates k_1 and k_2 were determined from a biexponential fit for the disappearance of A with time. Thus, the rate constants determined at different temperatures were fitted to Arrhenius and Eyring equations to extract the activation parameters, namely, log A, E_a, $\Delta H^{\ddagger}$, and $\Delta S^{\ddagger}$, cf. Table 3, for both racemization as well as thermal

Table 3. Activation Energy (E_a), Pre-Exponential Factor (A), $\Delta H^{\ddagger}$ and $\Delta S^{\ddagger}$, and Rate Constant for Racemization and Reversion/Ring Closure at 353 K as Determined by HPLC Analyses for a Representative *o*-Quinonoid Intermediate, i.e., 3BocQ

entry	parameters	inversion/racemization	thermal reversion
1	E_a (kcal mol^{-1})	31.07	28.06
2	logA	13.88	12.3
3	$\Delta H^{\ddagger}$ (kcal mol^{-1})	30.31	27.25
4	$\Delta S^{\ddagger}$ (cal K^{-1} mol^{-1})	2.5	−4.65
5	k (s^{-1})	0.54 × 10^{-5}	0.85 × 10^{-5}

reversion/ring closure. Indeed, the Arrhenius activation barriers for reversion of **3BocQ** thus extracted from the integrated equation above agree closely with those determined by time-dependent thermal reversion as followed by UV−vis absorption spectroscopy (Table 2). Further, the Arrhenius inversion/racemization barrier determined likewise is found to compare very well with those determined experimentally for analogous pentahelical systems that contain a methyl group at the C1 position.[36]

Helicity-Dependent Stabilization and Reversion of the Colored *o*-Quinonoid Intermediates at Graded Intervals of Temperature. The mechanism of photochromism of chromenes has been a subject of several investigations.[37−40] The current understanding is that the photoexcitation of chromenes results in C−O bond cleavage leading to the colored species, which are ascribed to the so-called *o*-quinonoid intermediates, cf. Scheme 3. The instantaneously formed CC isomer may undergo either rapid bond rotation to the TC isomer or collapse back to the precursor chromene. A two-photon absorption by the TC isomer has been shown to lead to the TT isomer, which may undergo C−C bond rotation to the CT isomer.[37−40] In general, the CC and CT isomers are discounted as being unimportant in the observed photochromism of chromenes at room temperature based on the consideration that the CC isomer must be very short-lived and that the population of CT isomers should be negligible due to steric strain in its geometry. Accordingly, the TC isomer is predominantly observed in laser-flash photolysis, while both TC and TT are observed under steady-state irradiation conditions; of course, the TC isomer corresponds generally to the predominant species.[41] In the backdrop of this knowledge, we attribute the species responsible for color observed upon photolysis of helical chromenes **1**−**4** to *o*-quinonoid intermediates. Indeed, the structure determinations by X-ray crystallography (Figure 4) unequivocally establish the colored species to be *o*-quinonoid intermediates.

dx.doi.org/10.1021/ja312027c | J. Am. Chem. Soc. 2013, 135, 6872−6884

Scheme 3. Mechanistic Details of Photochromism of Chromene (left) and the Behavior Observed for Helical Chromenes 1−4 (right)

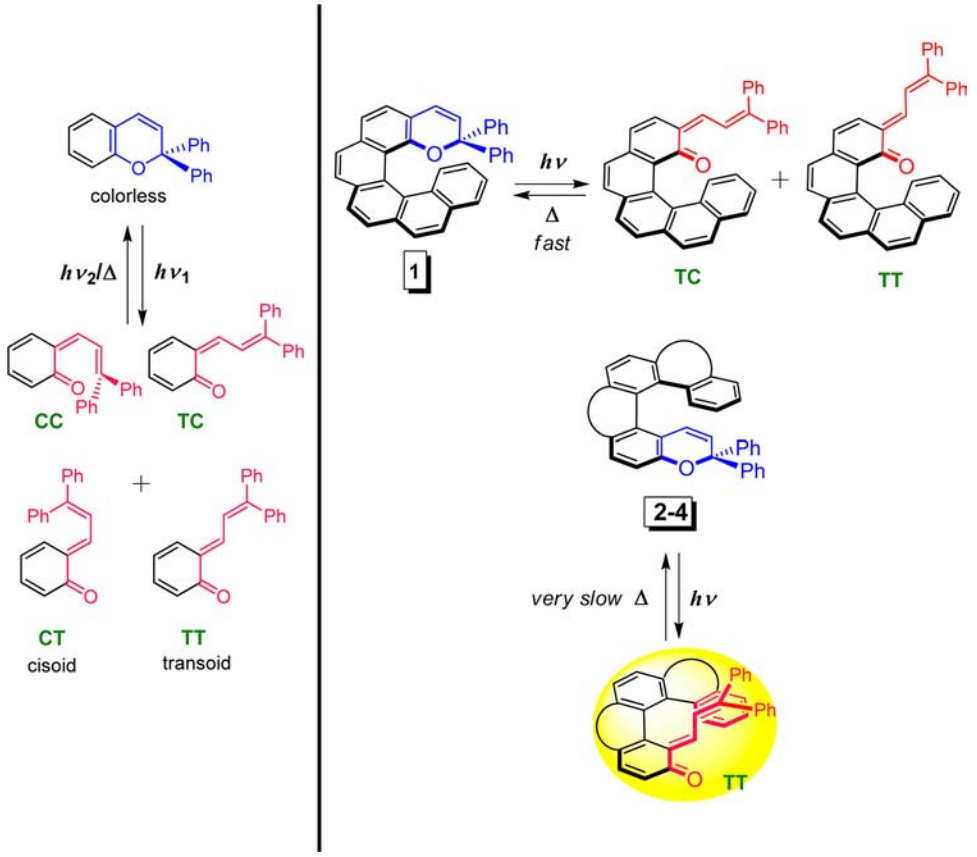

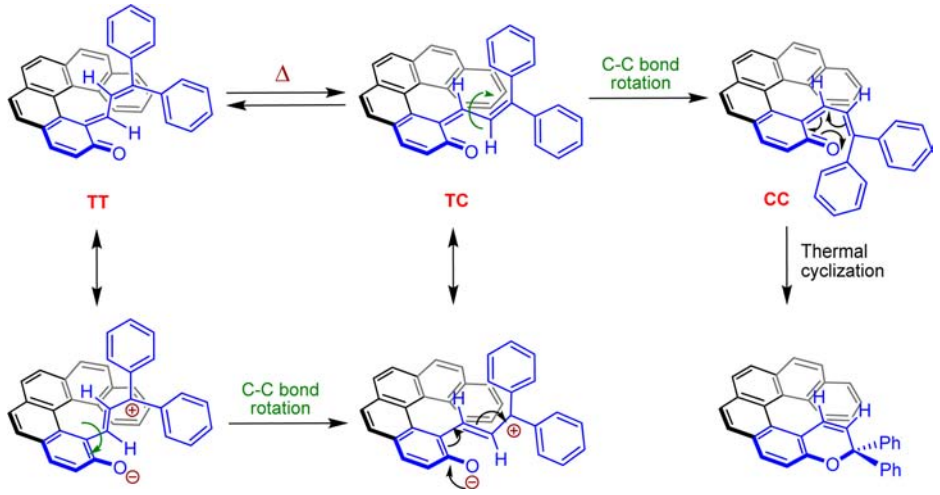

Figure 5. Necessary bond rotations that must occur for collapse of the TT isomers of the *o*-quinonoid intermediates to the corresponding colorless chromenes as shown for **2Q** as a representative case.

In line with the mechanistic picture described above, the photogenerated *o*-quinonoid intermediates of helical chromene **1** with its pyran oxygen located on the periphery of the helical scaffold exhibited decay kinetics that could be fitted to a biexponential function. The fast-decaying predominant component is attributed to the TC isomer, while the slow-decaying minor fraction is assigned to the TT isomer. The brick-red color was bleached within 2−3 min after exposure of the solution of **1** to UV radiation. In contrast, the color in the case of its regioisomeric chromene **2** was found to be highly persistent to permit isolation and characterization of the *o*-quinonoid intermediate (**2Q**), cf. Figure 4 and Scheme 3. The reversion behavior of the colored species of **1** is something that is typically observed for chromenes for which the *o*-quinonoid intermediates are stabilized by electronic or hydrogen-bonding interactions.[34,35,42,43] The question that springs up is: What is it that causes the stability of **2Q** to be so drastically different from that of **1Q**? The origin of observed differentiation in the persistence of the regioisomeric colored intermediates should

dx.doi.org/10.1021/ja312027c | *J. Am. Chem. Soc.* 2013, 135, 6872−6884

be traceable to the structural factors, which seemingly operate differently.

The X-ray crystal structures of **2Q**–**4Q** establish the geometry to be TT. We believe that the steric and electronic factors may influence mesomeric structures such that thermal equilibrium is possible via C–C bond rotations between the TC and TT isomers.[44] To reconcile the regio-differentiating thermal bleaching behavior of **1Q** and **2Q**, let us consider their structures in Scheme 3. In the TT and TC isomers of **1Q**, the diphenylvinyl moiety is disposed outward of the helical scaffold, while it is splayed over the internal curvature of the helical scaffold in **2Q**. For reversion of the TC and TT *o*-quinonoid intermediates to the colorless closed form, the diphenylvinyl moiety must undergo bond rotations. As one may readily decipher, the reversion to the colorless form should be easy in **1Q** due to lack of steric barrier for rotation of the diphenylvinyl moiety. In contrast, the TT isomer in the case of **2Q** should be fraught with a huge barrier enforced by the helical scaffold for its reversion.

As shown in Figure 5, the TT isomer must undergo bond rotation first to the TC isomer and close up to the chromene in the subsequent steps. In fact, collapse of the TC isomer to the chromene via CC isomer may be sterically accelerated. Thus, bond rotation in the TT isomer that leads to the TC isomer should determine the barrier for collapse of the *o*-quinonoid intermediate to the chromene. As can be seen from Figure 5, the diphenylvinyl moiety cannot easily undergo the required bond rotations to get ultimately to the CC isomer to revert to the colorless precursor. The TT isomer is evidently the most stable isomer in which the diphenyvinyl moiety is castled nicely within the helical arc. The recent theoretical calculations[44] show that the TT isomer is the most stable of all others even in systems that are devoid of steric factors. Thus, it is the operation of steric force—exerted by the helical scaffold in the *o*-quinonoid moiety—in **2Q** and lack of it in **1Q** that is the origin of extreme stability or rapid reversion, respectively.

This contrasting behavior exhibited by the regioisomeric intermediates of **1** and **2** in terms of persistence was indeed the basis for the design of heterohelical analogs **3** and **4**. The objective, as mentioned earlier, was to modulate the helicity of helical chromenes and examine the extent to which the persistence of the photogenerated colored intermediates is influenced. In **3** and **4**, location of the five-membered heterocyclic ring was envisaged to modify the helical arc and hence the steric force. Differences in the magnitudes of steric force extant in helical chromenes **2**–**4** can be assessed from d, θ, ψ_1, ψ_2, and φ_{total} described earlier. Accordingly smaller values of d and larger values of θ should imply severe steric crowding. As shown in Figure 1, the distance 'd' is lowest for **2** followed by **3Me** and **4Me**. The angle 'θ' is highest for **2** followed by **3Me** and **4Me**. In a similar manner, the other parameters, i.e., ψ_1, ψ_2, and φ_{total}, are highest for **2** and lowest for **4**. Thus, the photogenerated TT isomer should be expected to be more stable in **2** followed by that in **3Me** and **4Me** such that the thermal reversion is slowest for **2Q** followed by **3MeQ** and **4MeQ**. In complete agreement with this reasoning, the experimentally observed order of the activation barriers for reversion is: **2Q** > **3MeQ** > **4MeQ**. This is clearly borne out from the decay rates of **2Q**, **3MeQ**, and **4MeQ** at 80 °C, cf. entry 5, Table 2; of the three intermediates, **2Q** decays the slowest and **4MeQ** the fastest.

The chromenes **3Boc** and **4Boc** represent systems in which the electronic factors are superposed over steric factors. Replacement of methyl by Boc group diverts participation of the lone pair in the resonance structures of the photogenerated quinonoid intermediates so as to influence the stabilities of the latter. This electronic effect is glaring for the intermediates of **4MeQ** and **4BocQ** in which the nitrogen is proximate to the *o*-quinonoid moiety such that its contribution to resonance stabilization is significant in **4MeQ** and virtually none in **4BocQ**. As can be seen from Table 2, the activation barrier for **4BocQ** is significantly lesser than that for **4MeQ**. The lack of such resonance stabilization in the former is reflected in its rapid decay (entry 5, Table 2). It is noteworthy that the steric hindrance is relatively lower in **4MeQ** and **4BocQ** so that their thermal reversions to the colorless forms are faster than those of **2Q** and **3Q**. In contrast, the influence of similar electronic factors is not apparent for **3MeQ** and **3BocQ**; the activation barriers for reversion in these cases are comparable and so are the rates of their decay. In these cases, the nitrogen is evidently too far away from the *o*-quinonoid moiety for the electronic factors to become important.

Helicenes are inherently characterized by chirality and may undergo racemization.[45] The barriers for the latter are determined by the number of aromatic rings that the helicene is made up of[46] and the presence of substituents on the atoms of inner helicene.[36] The helical inversion may in principle compete with thermal reversion of the colored intermediates, i.e., **2Q**–**4Q**. Such a process occurring simultaneously might influence the bond rotations and favored configurations of the *o*-quinonoid intermediates on heating. The barriers for inversion/racemization as well as reversion to chromene determined for the resolved enantiomer of **3BocQ** described earlier show that the reversion occurs much faster than inversion/racemization. This should indeed be the case for **2Q** and **3MeQ** for which the activation barriers for thermal reversion are comparable. For these cases, the slow racemization should be expected to have no bearing on the conformational changes explored by the *o*-quinonoid intermediates during their reversion to chromenes. In contrast, for intermediates with low activation barriers for thermal reversions, i.e., **4MeQ** and **4BocQ**, the racemization is likely to compete efficiently with reversion.

Molecular Logic Gate Based on Photochromic Properties of the Helical Chromenes and Stimuli-Responsive Reversion of their Stable *o*-Quinonoid Intermediates. Construction of molecular-level electronic devices[47] is one of the chief goals in the contemporary chemistry of functional materials.[48−50] Molecular switches,[10,51] the chemical systems that undergo reversible changes under the influence of appropriate input, are exploited in the fabrication of miniaturized systems. The ultimate objective is to obviate the use of macroscopic semiconductors and develop molecular switches that mimic Boolean logic[52] conventions to permit electronic computing at the molecular level through encoding and decoding of binary digits, i.e., 0 and 1, in the form of input and output.

The photochromic phenomenon observed with helical chromenes in conjunction with thermal reversion of the colored intermediates allows, in principle, adaptation of **2**–**4** to logic operations. We found that the colored *o*-quinonoid intermediates can be readily reverted with visible radiation as well as H^+. Thus, one has four inputs, namely UV radiation (I_1), heat (I_2), H^+ (I_3), and visible radiation (I_4), and one output (O) described by the absorption at a chosen wavelength in the visible range. By defining an absorbance of <0.1 and >0.1 at 524

dx.doi.org/10.1021/ja312027c | J. Am. Chem. Soc. 2013, 135, 6872−6884

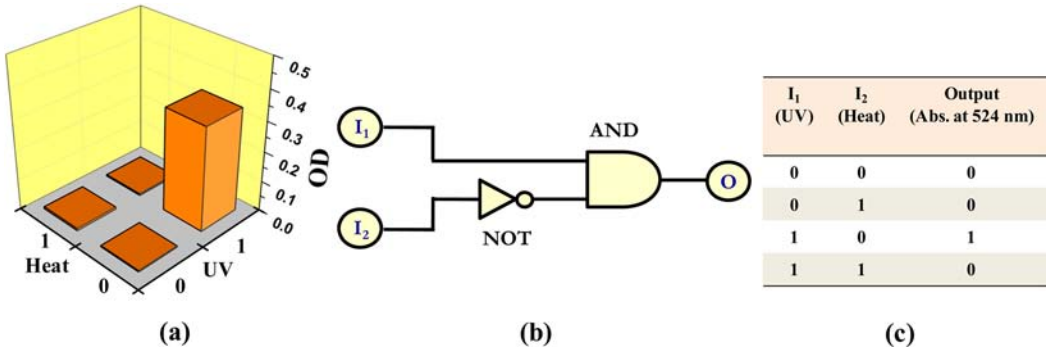

Figure 6. Representation of a two-state molecular switch based on INH logic function.

nm as corresponding to the output being 0 or 1, respectively, one deduces that the logic gate is 'on', i.e., $O = 1$, only when UV light is present ($I_1 = 1$) and all other inputs are absent ($I_2 = 0$, $I_3 = 0$, $I_4 = 0$). Further, when the UV radiation is absent ($I_1 = 0$) or when any of the inputs I_2–I_4 is present simultaneously with I_1, the absorbance at 524 nm would be <0.1 such that $O = 0$. Thus, the photochromic helical chromenes **2**–**4** represent two-state molecular switches with an overall INHIBIT (INH) logic gate function. The functioning of the molecular switch with UV and heat as the input is shown in Figure 6 for the helical chromene **2** along with the truth table for the INH logic operation. Thus, the photo- and thermoresponsive helical chromenes **2**–**4** should constitute novel additions to the gamut of molecular logic gates. A variety of logic operations[53] have been fabricated at the molecular level. It turns out that the logic operation INHIBIT[54] has been explored in a range of applications.[55,56] A new and exciting dimension is the application of INHIBIT in photonic materials with light as an input.

Photochromism of Helical Chromenes and Implications for Application as Molecular Switches in Optical Data Storage. Photochromic diarylpyrans (chromenes), spiropyrans, and spirooxazines[32,57] have gained lots of importance in terms of their applications in ophthalmic lenses[31,32] and liquid crystals.[57] The advantages with these photochromes are the ease of synthetic accessibility, structural variability, high quantum yields of photocoloration, high fatigue resistance, and very high two-photon cross section. Insofar as their application in optical data storage devices[57,58] is concerned, the major disadvantage is that the energy barrier for thermal reversion of the photogenerated colored forms is very low.[33,59] This serious drawback continues to curtail their application to long-term storage of light-written information in particular. Indeed, bistability of photochromic compounds is a fundamental requirement in 'photochemical erasable memory'.[60] In spite of a large number of modifications toward improving the kinetic parameters for thermal reversion of the photogenerated colored merocyanine forms, chromenes, spiropyrans, and spirooxazines appear to fail in rivaling the bistability observed with diarylethylenes[58] and fulgides.[61] Only few instances of stabilization[43,62,63] of colored merocyanines by electronic delocalization, dipole interactions, hydrogen bonding, etc. are known in contrast to a number of reports that exemplify the isolation and characterization of photogenerated colored intermediates of diarylethylenes[64] and fulgides.[65]

In light of the aforementioned notorious limitation with thermal instability of the colored forms of chromenes/spiropyrans/spirooxzines, the exceptional stability of the *o*-quinonoid intermediates of helical chromenes **2**–**4** engineered via sterics built into the helical scaffold via rational design is remarkable. For example, the activation parameters for reversion of the colored form of **2Q** point to a half-life ≃ 46 years at 298 K, which renders them as being equivalent to well-acknowledged photochromic materials, namely, diarylethylenes[59] (lifetime ≃ 45 years at 298 K). The longest lifetimes known heretofore for some of the best examples of spiropyrans, spirooxazines, and fulgides are ≃7 d, 1.4 h, and ≃3 d, respectively, at 298 K.[59] Thus, the stability of the photogenerated colored intermediates observed herein for the helical chromenes **2**–**4** should confer the latter with unparalleled utility in light-written data storage devices, more so in view of the fact that the optical information can be read out easily with other stimuli, such as H^+ and visible radiation, cf. Figure 7.

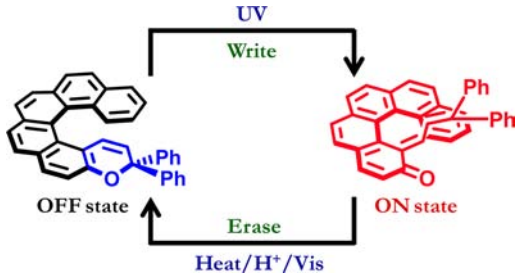

Figure 7. Read-out of light-written information as applied to optical data storage.

■ CONCLUSIONS

Photolysis of rationally designed regioisomeric helical chromenes **1** and **2** is shown to lead to colored reactive intermediates in both cases. While the photogenerated colored species decay quite rapidly in general, they are found to be longer lived in the case of **1** and highly persistent in the case of **2**; the calculated half-life is 46 years. The remarkable stability of the intermediate **2Q** permitted characterization by X-ray crystallography. Structural analyses reveal that the steric force inherent to the helical scaffold is the origin of stability as well as differentiation in the persistence of **1Q** and **2Q**. In the latter, the diphenylvinyl moiety gets splayed over the helical scaffold, whereby it is fraught with a huge steric strain to undergo required bond rotations to regenerate the precursor chromene. Otherwise, reversion is found to occur at high temperatures. Based on the helicity-dependent steric barrier for thermal reversion, azahelical chromenes **3** and **4** that are analogs of **2** and differ in terms of the magnitude of helicity were designed

dx.doi.org/10.1021/ja312027c | J. Am. Chem. Soc. 2013, 135, 6872–6884

in pursuit of *o*-quinonoid intermediates with graded activation barriers. The helical chromenes **3** and **4** were also found to exhibit photochromism akin to **2** such that their respective photogenerated intermediates (**3Q** and **4Q**) are also isolated and structurally characterized. The thermal reversion barriers of **2Q**−**4Q** are shown to correlate uniquely with the helical turn, which decisively determines the steric force. The exploitation of helicity is thus demonstrated to develop a novel set of photoresponsive molecular systems **2**−**4** that lead to colored *o*-quinonoid intermediates of varying stabilities and revert thermally at graded intervals of temperature. It is shown that the photochromic phenomena of **2**−**4** in conjunction with the response of their intermediates **2Q**−**4Q** to external stimuli, such as acid, heat, and visible radiation allow development of molecular logic gates with INH function. To the best of our knowledge, exploitation of the helicity in a rational manner to stabilize reactive intermediates and thus modulate functional behavior is unprecedented.

EXPERIMENTAL SECTION

General Aspects. ^{1}H and ^{13}C NMR spectra were recorded on JEOL (400 and 500 MHz) spectrometers in $CDCl_3/C_6D_6/CD_3CN$ as a solvent. The ESI mass spectra were recorded on Waters ^{Q}TOF machine. UV−vis absorption spectra were recorded using a Shimadzu UV-1800 spectrophotometer. Dry tetrahydrofuran (THF) and toluene were freshly distilled over sodium prior to use. All the reactions were monitored by analytical thin layer chromatography (TLC) using commercial aluminum sheets precoated with silica gel. Chromatography was conducted on silica gel (Acme, Mumbai, 60−120 mesh). All the commercial chemicals were used as received.

Synthesis of Helical Chromenes. The carbohelical chromenes **1** and **2** were synthesized from precursor helical coumarins via Grignard reaction followed by dehydration. The helical coumarins were in turn prepared by oxidative photocyclization of the diarylolefins accessed by Wittig olefination, cf. Supporting Information. The azahelical chromenes **3Me** and **3Boc** were prepared by subjecting the suitably functionalized phenols to cyclocondensation with 1,1-diphenylpropargyl alcohol in the presence of PPTS as a catalyst in dry 1,2-dichloroethane at reflux. The required hydroxy-substituted helical carbazole derivatives were prepared by a sequence of reactions involving Wittig olefination, oxidative cyclization, and Dakin reaction, cf. Supporting Information. Similarly, chromenes **4Me** and **4Boc** were prepared starting from 3,6-diformylcarbazole by an analogous sequence of reactions mentioned above. The phenols were then transformed to the chromenes by reacting with 1,1-diphenylpropargyl alcohol using PPTS as a catalyst. All the helical chromenes were comprehensively characterized by IR, NMR, and mass analyses.

Representative Procedure for Grignard Reaction Followed by Cyclization: Synthesis of Carbohelical Chromenes 1 and 2. To a stirred solution of excess of phenylmagnesium bromide (0.33 g, 1.8 mmol) in dry THF at 0 °C was added a solution of helical coumarin, i.e., phenanthro[9,10-*k*]-3*H*-naphthopyran-3-one (0.10 g, 0.3 mmol), in THF (3 mL) under nitrogen gas atmosphere. After stirring for 1 h at room temperature, the reaction mixture was cooled, quenched with dil H_2SO_4, and stirred at room temperature for 1 h. The resultant reaction mixture was extracted with ethyl acetate. The combined organic extract was washed with brine solution, dried over anhyd sodium sulfate, filtered, and evaporated. The crude product obtained was purified by silica gel column chromatography to afford chromene **2** as a pale-yellow crystalline solid (0.05 g, 34% yield). A similar protocol was adopted to synthesize **1** (15% yield) from phenanthro[9,10-*k*]-2*H*-naphthopyran-2-one.

Carbohelical Chromene 1. Off-white solid, yield 15%; mp 174−177 °C; IR (film) cm^{-1} 3052, 2925, 2835, 1447; ^{1}H NMR ($CDCl_3$, 500 MHz) δ 6.06 (d, J = 9.5 Hz, 1H), 6.18 (d, J = 7.4 Hz, 2H), 6.43 (d, J = 7.5 Hz, 2H), 6.68−6.71 (m, 2H), 6.74 (d, J = 9.4 Hz, 1H), 6.81 (t, J = 7.4 Hz, 1H), 6.96−7.00 (m, 2H), 7.08 (t, J = 7.4 Hz, 1H), 7.21−7.30 (m, 2H), 7.43 (t, J = 7.4 Hz, 1H), 7.49 (d, J = 8.0 Hz, 1H), 7.67 (d, J = 8.6 Hz, 1H), 7.69−7.73 (m, 3H), 7.79 (d, J = 8.6 Hz, 1H), 7.85 (d, J = 8.0 Hz, 1H), 7.93 (d, J = 8.3 Hz, 1H), 8.31 (d, J = 8.3 Hz, 1H); ^{13}C NMR ($CDCl_3$, 125 MHz) δ 82.9, 119.8, 122.7, 123.2, 124.3, 124.5, 124.9, 125.4, 125.6, 125.7, 126.0 (×2), 126.4 (×2), 126.7 (×2), 126.8, 126.9, 127.16 (×2), 127.24, 127.5 (×2), 127.9, 129.6, 130.0, 130.5, 131.4, 132.5, 133.3, 133.9, 143.6, 144.3, 149.7; ESI-MS$^+$ m/z calcd for $C_{37}H_{25}O$, 485.1905 [M + H]; found, 485.1902.

Carbohelical Chromene 2. Pale-yellow crystalline solid, yield 34%; mp 151−153 °C; IR (film) cm^{-1} 3056, 2924, 2853, 1490, 1446; ^{1}H NMR ($CDCl_3$, 500 MHz) δ 5.41 (d, J = 10.3 Hz, 1H), 5.86 (d, J = 10.3 Hz, 1H), 6.10 (t, J = 8.0 Hz, 1H), 7.10−7.22 (m, 6H), 7.31 (d, J = 6.9 Hz, 2H), 7.35−7.48 (m, 4H), 7.68 (d, J = 8.6 Hz, 1H), 7.72 (d, J = 8.0 Hz, 1H), 7.80 (d, J = 8.0 Hz, 1H), 7.83 (d, J = 8.6 Hz, 1H), 7.84−7.94 (m, 5H); ^{13}C NMR ($CDCl_3$, 125 MHz) δ 81.5, 116.1, 117.7, 122.6, 123.4, 123.7, 124.0, 125.5, 125.7, 126.0, 126.6, 127.0 (×2), 127.1 (×2), 127.3, 127.39, 127.45, 128.0 (×2), 128.1 (×2), 128.4, 128.6, 129.0, 129.7, 130.5, 130.6, 131.3, 133.6, 144.4, 146.1, 151.1; ESI-MS$^+$ m/z calcd for $C_{37}H_{25}O$, 485.1905 [M + H]; found, 485.1908.

Representative Procedure for Cyclocondensation of Phenols with 1,1-Diphenylpropargyl Alcohol: Synthesis of Azahelical Chromene 3Me. An oven-dried round-bottom flask was charged with 2-hydroxy-9-methyl-9*H*-naphtho[2,1-*c*]carbazole (0.90 g, 3.03 mmol), 1,1-diphenylprop-2-yn-1-ol (1.26 g, 6.06 mmol), and a catalytic amount of PPTS (0.04 g, 5 mol %) under a nitrogen gas atmosphere, and dry 1,2-dichloroethane (40 mL) was introduced. The contents were heated at reflux for 18−24 h. After this period, the reaction mixture was cooled and washed with saturated Na_2CO_3 solution, and the organic matter was extracted with chloroform (30 mL ×3). The combined extract was dried over anhyd. Na_2SO_4, filtered, and evaporated to yield the crude compound. Further purification by silica-gel column chromatography using 2.5% ethyl acetate in pet ether afforded the azahelical chromene **3Me** as a colorless crystalline material in 76% yield; mp 210−212 °C; IR (KBr) cm^{-1} 3401, 2975, 1702, 1615, 1371; ^{1}H NMR ($CDCl_3$, 500 MHz) δ 3.97 (s, 3H), 5.77 (d, J = 10.1 Hz, 1H), 6.39 (t, J = 7.9 Hz, 1H), 6.79 (d, J = 10.1 Hz, 1H), 7.22−7.33 (m, 6H), 7.39−7.47 (m, 3H), 7.51−7.57 (m, 4H), 7.66 (d, J = 8.3 Hz, 1H), 7.69 (d, J = 7.7 Hz, 2H), 7.72 (d, J = 8.6 Hz, 1H), 7.86 (d, J = 8.6 Hz, 1H), 7.90 (d, J = 8.6 Hz, 1H); ^{13}C NMR ($CDCl_3$, 125 MHz) δ 29.4, 81.9, 107.8, 109.9, 117.1, 117.2, 118.2, 119.0, 122.3, 123.8, 124.0, 124.5, 124.6, 125.0 (×2), 126.4, 126.9 (×2), 127.3 (×2), 127.4, 127.5, 127.8, 128.1 (×2), 128.2 (×2), 128.3, 128.4, 129.4, 129.5, 139.9, 140.0, 140.5, 144.4, 151.1; ESI-MS$^+$ m/z calcd for $C_{36}H_{26}NO$, 488.2014 [M + H]; found, 488.2019.

Azahelical Chromene 3Boc. Colorless solid, yield 79%; mp 178−180 °C; IR (KBr) cm^{-1} 3057, 2924, 1724, 1457, 1313; ^{1}H NMR ($CDCl_3$, 500 MHz) δ 1.82 (s, 9H), 5.78 (d, J = 10.3 Hz, 1H), 6.31 (t, J = 8.0 Hz, 1H), 6.70 (d, J = 10.1 Hz, 1H), 7.24−7.29 (m, 7H), 7.44−7.48 (m, 3H), 7.54 (t, J = 7.2 Hz, 2H), 7.62−7.64 (m, 3H), 7.87 (d, J = 2.3 Hz, 1H), 7.89 (d, J = 2.6 Hz, 1H), 8.29 (d, J = 8.3 Hz, 1H), 8.66 (d, J = 8.6 Hz, 1H); ^{13}C NMR ($CDCl_3$, 125 MHz) δ 28.4 (×3), 82.1, 84.2, 115.2, 116.5, 117.2, 117.4, 122.1, 122.6, 122.8, 123.3, 123.4, 124.6, 124.8, 125.6, 125.9, 126.8 (×2), 127.1, 127.3 (×2), 127.4, 127.61, 127.65, 128.1 (×2), 128.4 (×2), 129.3, 129.7, 130.8, 137.4, 137.7, 144.4, 146.0, 151.1, 151.3; ESI-MS$^+$ m/z calcd for $C_{40}H_{32}NO_3$, 574.2382 [M + H]; found, 574.2381.

Azahelical Chromene 4Me. Colorless solid, yield 78%; mp 104−106 °C; IR (KBr) cm^{-1} 3054, 2920, 2850, 1729, 1589, 1435, 1263; ^{1}H NMR ($CDCl_3$, 500 MHz) δ 3.93 (s, 3H), 5.84 (d, J = 9.5 Hz, 1H), 6.65 (d, J = 9.8 Hz, 1H), 7.28−7.32 (m, 4H), 7.34−7.41 (m, 5H), 7.49−7.52 (m, 2H), 7.56 (t, J = 7.1 Hz, 1H), 7.60 (d, J = 8.6 Hz, 1H), 7.72 (d, J = 8.6 Hz, 1H), 7.82−7.85 (m, 4H), 7.91 (d, J = 7.7 Hz, 1H), 8.57 (d, J = 8.3 Hz, 1H); ^{13}C NMR ($CDCl_3$, 125 MHz) δ 29.7, 81.3, 109.4, 109.8, 115.0, 115.1, 116.1, 121.2, 123.8, 123.9, 124.3, 126.2, 126.3, 126.8 (×2), 126.9, 127.1, 127.14, 127.17, 127.19, 127.5, 127.6 (×2), 127.9, 128.1 (×2), 128.7, 129.8, 132.7, 136.4, 141.5, 144.4, 146.0, 146.8; ESI-MS$^+$ m/z calcd for $C_{36}H_{26}NO$, 488.2014 [M + H]; found, 488.2011.

Azahelical Chromene 4Boc. Pale yellow, yield 69%; mp 88−90 °C; IR (KBr) cm^{-1} 3053, 2969, 2925, 1724, 1664, 1447, 1315; ^{1}H NMR ($CDCl_3$, 500 MHz) δ 1.78 (m, 9H), 5.79 (d, J = 9.8 Hz, 1H),

dx.doi.org/10.1021/ja312027c | J. Am. Chem. Soc. 2013, 135, 6872−6884

6.40 (d, J = 9.8 Hz, 1H), 7.13−7.16 (m, 1H), 7.22−7.30 (m, 4H), 7.34−7.39 (m, 3H), 7.49−7.54 (m, 3H), 7.71 (d, J = 7.7 Hz, 2H), 7.75 (d, J = 8.6 Hz, 1H), 7.79 (d, J = 8.6 Hz, 1H), 7.85 (d, J = 8.6 Hz, 1H), 7.89 (d, J = 7.7 Hz, 1H), 8.31 (d, J = 2.2 Hz, 1H), 8.32 (d, J = 3.4 Hz, 1H), 8.56 (d, J = 8.6 Hz, 1H); ^{13}C NMR ($CDCl_3$, 125 MHz) δ 28.4 (×3), 81.4, 84.3, 115.4, 115.5, 115.8, 117.2, 119.2, 124.3, 124.5, 124.9, 125.0, 125.7, 126.3, 126.4, 126.5, 126.8 (×2), 127.1, 127.3 (×2), 127.4 (×2), 127.6, 127.8, 127.9, 128.1 (×3), 129.3, 130.0, 132.4, 133.6, 139.7, 144.1, 145.7, 148.9, 150.7; ESI-MS$^+$ m/z calcd for $C_{40}H_{32}NO_3$, 574.2382 [M + H]; found, 574.2381.

Representative Procedure for Preparative Scale Photolysis of Chromenes: Isolation of *o*-Quinonoid Intermediates. A solution of carbohelical chromene **2**, a representative case, in freshly distilled DCM (~10^{-4}−10^{-5} M) was purged with nitrogen gas for 20 min. The resulting solution was irradiated in a Luzchem photoreactor fitted with 350 nm lamps for ~30 min. The progress of the reaction was monitored by TLC analysis, which was characterized by the appearance of dark-red color. The photolysate was stripped off the solvent under reduced pressure at room temperature, and the resulting solid was subjected to silica-gel (neutral) column chromatography to afford pure **2Q** as a dark-red solid. IR (KBr) cm^{-1} 3053, 2923, 2853, 1646, 1536; ^{1}H NMR (CD_3CN, 500 MHz) δ 5.19 (d, J = 11.7 Hz, 1H), 6.00 (d, J = 7.7 Hz, 2H), 6.21 (d, J = 11.7 Hz, 1H), 6.39 (d, J = 9.7 Hz, 1H), 6.51 (d, J = 7.7 Hz, 2H), 7.10−7.18 (m, 4H), 7.23 (t, J = 7.4 Hz, 1H), 7.27−7.30 (m, 1H), 7.37 (d, J = 8.5 Hz, 1H), 7.41−7.45 (m, 1H), 7.60−7.64 (m, 2H), 7.69 (d, J = 8.3 Hz, 1H), 7.73 (d, J = 7.7 Hz, 1H), 7.79 (d, J = 9.4 Hz, 1H),7.87−7.89 (m, 2H), 7.99 (d, J = 7.7 Hz, 1H), 8.14 (d, J = 8.3 Hz, 1H); ^{13}C NMR (C_6D_6, 125 MHz) δ 124.0, 125.7, 125.8, 126.7, 127.0, 127.1, 127.2, 128.2, 128.4, 128.7, 129.2, 130.0, 131.0, 131.9, 132.7, 133.8, 134.1, 137.6, 138.0, 138.1, 141.6, 143.0. 152.0, 188.6; ESI-MS$^+$ m/z calcd for $C_{37}H_{25}O$, 485.1905[M + H]; found, 485.1903.

***o*-Quinonoid Intermediate 3MeQ.** Dark-red crystalline solid; IR (film) cm^{-1} 2920, 2850, 1729, 1460, 1370; ^{1}H NMR (C_6D_6, 500 MHz) δ 2.97 (s, 3H), 6.07 (d, J = 12.2 Hz, 1H), 6.37 (dd, J_1 = 8.4 Hz, J_2 = 1.2 Hz, 2H), 6.45−6.46 (m, 2H), 6.47 (d, J = 9.4 Hz, 1H), 6.70 (t, J = 7.9 Hz, 2H), 6.78−6.81 (m, 1H), 6.95 (dd, J_1 = 7.0 Hz, J_2 = 2.7 Hz, 1H), 7.00−7.12 (m, 6H), 7.27−7.32 (m, 2H), 7.49 (d, J = 12.2 Hz, 1H), 7.63 (d, J = 8.9 Hz, 1H), 7.70 (d, J = 7.9 Hz, 1H), 8.53 (dd, J_1 = 6.1 Hz, J_2 = 1.9 Hz, 1H); ^{13}C NMR ($CDCl_3$, 125 MHz) δ 29.7, 106.2, 108.9, 109.1, 111.8, 117.6, 118.1, 118.5, 119.3, 123.9, 124.1, 124.3, 124.7, 126.8, 126.9, 127.2 (×2), 127.5, 127.6 (×2), 127.8 (×2), 127.9, 128.1 (×2), 128.3, 128.9, 130.1 (×2), 130.5, 131.4, 138.2, 139.6, 144.1, 152.5, 190.9; ESI-MS$^+$ m/z calcd for $C_{36}H_{26}NO$, 488.2014 [M + H]; found, 488.2018.

***o*-Quinonoid Intermediate 3BocQ.** Dark-red solid; IR (KBr) cm^{-1} 2917, 2849, 1728, 1460, 1310; ^{1}H NMR ($CDCl_3$, 500 MHz) δ 1.70 (s, 9H), 5.88 (d, J = 12.3 Hz, 1H), 6.35 (d, J = 7.2 Hz, 1H), 6.49−6.51 (m, 3H), 6.98 (d, J = 12.3 Hz, 1H), 7.02−7.05 (m, 2H), 7.12 (t, J = 7.2 Hz, 1H), 7.19−7.29 (m, 4H), 7.36 (t, J = 7.5 Hz, 1H), 7.44 (t, J = 7.2 Hz, 1H), 7.53 (d, J = 8.1 Hz, 1H), 7.64 (d, J = 9.7 Hz, 1H). 7.88 (d, J = 9.2 Hz, 1H), 7.92 (d, J = 8.1 Hz, 1H), 7.96 (d, J = 8.0 Hz, 1H), 8.26 (d, J = 8.3 Hz, 1H), 8.59 (d, J = 8.9 Hz, 1H); ^{13}C NMR ($CDCl_3$, 125 MHz) δ 29.7 (×3), 84.4, 115.8, 117.6, 120.3, 122.2, 123.7, 124.4, 125.1, 125.5, 125.8, 125.9, 127.2 (×2), 127.7, 127.9 (× 3), 128.0, 128.1, 128.4, 128.6, 129.8, 130.0 (×2), 131.1, 131.7, 137.5, 137.72, 137.77, 138.6, 140.8, 140.9, 143.7, 150.6, 153.5, 190.3; ESI-MS$^+$ m/z calcd for $C_{40}H_{32}NO_3$, 574.2382 [M + H]; found, 574.2386.

***o*-Quinonoid Intermediate 4MeQ.** Dark-red crystalline solid; IR (neat) cm^{-1} 3053, 2923, 2853, 1646, 1536; ^{1}H NMR ($CDCl_3$, 500 MHz) δ 4.02 (s, 3H), 5.97 (d, J = 12.6 Hz, 1H), 6.01 (d, J = 7.7 Hz, 2H), 6.40 (d, J = 9.7 Hz, 1H), 6.87−6.90 (m, 4H), 7.03−7.05 (m, 1H), 7.29−7.35 (m, 4H), 7.44−7.47 (m, 1H), 7.49−7.52 (m, 1H), 7.59 (d, J = 10.0 Hz, 1H), 7.63−7.67 (m, 3H), 7.85 (d, J = 8.6 Hz, 2H), 8.21 (d, J = 8.3 Hz, 1H); ^{13}C NMR ($CDCl_3$, 125 MHz) δ 29.7, 110.5, 117.6, 119.7, 125.1, 125.5, 125.7, 125.9, 126.04, 126.09, 126.1, 126.3, 127.3 (×2), 127.5 (×2), 127.6, 127.7, 127.8, 127.9 (×2), 128.61, 128.69, 128.7, 130.4 (×2), 132.1, 132.5, 135.5, 138.1, 138.5, 139.7, 140.2, 150.7, 189.9; ESI-MS$^+$ m/z calcd for $C_{36}H_{26}NO$ 488.2014 [M + H]; found, 488.2018.

***o*-Quinonoid Intermediate 4BocQ.** Dark-red crystalline solid. IR (neat) cm^{-1} 3053, 2923, 2853, 1646, 1536; ^{1}H NMR ($CDCl_3$, 500 MHz) δ 1.78 (s, 9H), 5.78 (d, J = 9.8 Hz, 1H), 6.40 (d, J = 9.8 Hz, 1H), 7.15 (t, J = 7.0 Hz, 1H), 7.21−7.31 (m, 5H), 7.33−7.39 (m, 3H), 7.46−7.58 (m, 3H), 7.71 (d, J = 7.4 Hz, 2H), 7.74 (d, J = 8.6 Hz, 1H), 7.78 (d, J = 8.6 Hz, 1H), 7.84 (d, J = 8.9 Hz, 1H), 7.88 (d, J = 7.9 Hz, 1H), 8.31 (d, J = 9.2 Hz, 1H), 8.56 (d, J = 8.9 Hz, 1H); ^{13}C NMR ($CDCl_3$, 125 MHz) δ 28.4, 84.3, 115.4, 115.5, 115.8, 117.2, 119.2, 121.5, 124.3, 124.5, 124.9, 125.0, 125.7, 126.3, 126.4, 126.5, 126.8, 127.4, 127.6, 127.8, 127.9, 128.0, 128.4, 129.2, 130.0, 130.2, 132.4, 133.6, 139.7, 144.1, 145.6, 148.9, 150.7, 185.8; ESI-MS$^+$ m/z calcd for $C_{40}H_{32}NO_3$, 574.2382 [M + H]; found, 574.2387.

X-ray Structure Determinations. The X-ray diffraction intensity data collection for the crystals of **1**, **2**, **3Me**, and **4Me** and the *o*-quinonoid intermediates, i.e., **2Q**, **3BocQ**, and **4MeQ**, was carried out at 100 K on a Bruker Nonius SMART APEX CCD detector system with Mo-sealed Siemens ceramic diffraction tube (λ = 0.7107 Å) and a highly oriented graphite monochromator operating at 50 kV and 30 mA. Subsequently, the data were collected in a hemisphere mode and processed with Bruker SAINTPLUS. Empirical absorption correction was made using Bruker SADABS. The structure was solved in each case by direct methods using SHELXL package and refined by full matrix least-squares method based on F^2 using SHELX-97 program. The hydrogens were largely located from difference Fourier maps, and those that could not be identified were fixed geometrically. Hydrogens were treated as riding on their nonhydrogens and refined isotropically, while all nonhydrogens were subjected to anisotropic refinement. The X-ray crystallographic coordinates for all the structures have been deposited at the Cambridge Crystallographic Data Centre (CCDC). The deposition numbers are CCDC 901784 (for **1**), CCDC 901785 (for **2**), CCDC 901786 (for **2Q**), CCDC 901787 for (**3BocQ**), CCDC 901788 for (**3Me**), CCDC 901789 for (**4Me**), and CCDC 901790 for (**4MeQ**). These data can be obtained free of charge (http://www.ccdc.cam.ac.uk/data_request/cif). Details of crystal data and refinement are given in the Supporting Information.

■ ASSOCIATED CONTENT

Ⓢ Supporting Information

Synthesis of starting materials and their spectral data, ^{1}H and ^{13}C NMR spectra of all the compounds, details of the determination of kinetic and thermodynamic parameters, absorption spectra, logic gate truth table, and tables of crystal data. This material is available free of charge via Internet at http://pubs.acs.org.

■ AUTHOR INFORMATION

Corresponding Author

moorthy@iitk.ac.in

Notes

The authors declare no competing financial interest.

■ ACKNOWLEDGMENTS

J.N.M. is thankful to Council of Scientific and Industrial Research (CSIR), India for funding. S.M. and A.M. are grateful to CSIR for senior and junior research fellowships, respectively.

■ REFERENCES

(1) *Classics in Hydrocarbon Chemistry*; Hopf, H., Ed.; Wiley-VCH: Weinheim, 2000.

(2) *Fascinating Molecules in Organic Chemistry*; Voegtle, F., Ed.; Wiley and Sons: New York, 1992.

(3) Dickerson, R. E.; Drew, H. R.; Conner, B. N.; Wing, R. M.; Fratini, A. V.; Kopka, M. L. *Science* **1982**, *216*, 475.

(4) Goriely, A.; Tobar, M. *Phys. Rev. Lett.* **1998**, *80*, 1564.

(5) *The Genome Analysis Centre (TGAC)*; TGAC: Norwich, U.K.; www.tgac.ac.uk/outreach/spotted-DNA-from-around-the-world/.

(6) (a) Newman, M.; Ednicer, D. *J. Am. Chem. Soc.* **1956**, *78*, 4765. (b) Martin, R. H. *Angew. Chem., Int. Ed.* **1974**, *13*, 649.
(7) (a) *Functional Organic Materials: Syntheses, Strategies and Applications*; Mueller, T. J. J., Bunz, U. H. F., Eds.; Wiley-VCH: Germany, 2007. (b) Shen, Y.; Chen, C.-F. *Chem. Rev.* **2012**, *112*, 1463. (c) Urbano, A. *Angew. Chem., Int. Ed.* **2003**, *42*, 3986.
(8) Weix, D. J.; Dreher, S. D.; Katz, T. J. *J. Am. Chem. Soc.* **2000**, *122*, 10027.
(9) Li, M.; Lu, H. Y.; Liu, R. L.; Chen, J. D.; Chen, C. F. *J. Org. Chem.* **2012**, *77*, 3670.
(10) Wigglesworth, T. J.; Sud, D.; Norsten, T. B.; Lekhi, V. S.; Branda, N. R. *J. Am. Chem. Soc.* **2005**, *127*, 7272.
(11) Tanaka, K.; Osuga, H.; Kitahara, Y. *J. Org. Chem.* **2002**, *67*, 1795.
(12) Kelly, T. R.; Cai, X.; Damkaci, F.; Panicker, S. B.; Tu, B.; Bushell, S. M.; Cornella, I.; Piggott, M. J.; Salives, R.; Cavero, M.; Zhao, Y.; Jasmin, S. *J. Am. Chem. Soc.* **2007**, *129*, 376.
(13) Fuchter, M. J.; Schaefer, J.; Judge, D. K.; Wardzinski, B.; Weimar, M.; Krossing, I. *Dalton Trans.* **2012**, *41*, 8238.
(14) Tagami, K.; Tsukada, M.; Wada, Y.; Iwasaki, T.; Nishide, H. *J. Chem. Phys.* **2003**, *119*, 7491.
(15) Field, J. E.; Muller, G.; Riehl, J. P.; Venkataraman, D. *J. Am. Chem. Soc.* **2003**, *125*, 11808.
(16) Sooksimuang, T.; Mandal, B. K. *J. Org. Chem.* **2003**, *68*, 652.
(17) Shi, L.; Liu, Z.; Dong, G.; Duan, L.; Qiu, Y.; Jia, J.; Guo, W.; Zhao, D.; Cui, D.; Tao, X. *Chem.—Eur. J.* **2012**, *18*, 8092.
(18) Verbiest, T.; Elshocht, S. V.; Persoons, A.; Nuckolls, C.; Phillips, K. E.; Katz, T. J. *Langmuir* **2001**, *17*, 4685.
(19) Shcherbina, M. A.; Zeng, X. −B.; Tadjiev, T.; Ungar, G.; Eichhorn, S. H.; Phillips, K. E. S.; Katz, T. Z. *Angew. Chem., Int. Ed.* **2009**, *48*, 7837.
(20) Dai, Y.; Katz, T. J.; Nichols, D. A. *Angew. Chem., Int. Ed.* **1996**, *35*, 2109.
(21) Xu, Y.; Zhang, Y. X.; Sugiyama, H.; Umano, T.; Osuga, H.; Tanaka, K. *J. Am. Chem. Soc.* **2004**, *126*, 6566.
(22) Shinohara, K.; Sannohe, Y.; Kaieda, S.; Tanaka, K.; Osuga, H.; Tahara, H.; Xu, Y.; Kawase, T.; Bando, T.; Sugiyama, H. *J. Am. Chem. Soc.* **2010**, *132*, 3778.
(23) Feringa, B. L.; van Delden, R. A.; Koumura, N.; Geertsema, E. M. *Chem. Rev.* **2000**, *100*, 1789.
(24) Graule, S.; Rudolph, M.; Vanthuyne, N.; Autschbach, J.; Roussel, C.; Crassous, J.; Réau, R. *J. Am. Chem. Soc.* **2009**, *131*, 3183.
(25) Sato, I.; Yamashima, R.; Kadowaki, K.; Yamamoto, J.; Shibata, T.; Soai, K. *Angew. Chem., Int. Ed.* **2001**, *40*, 1096.
(26) Takenaka, N.; Chen, J.; Captain, B.; Sarangthem, R. S.; Chandrakumar, A. *J. Am. Chem. Soc.* **2010**, *132*, 4536.
(27) Helicenoid is a term that is seemingly used to describe molecular structures that are helical in shape (i.e., helicene-like) but are made up of noncondensed aromatics.
(28) Okuyama, T.; Tani, Y.; Miyake, K.; Yokoyama, Y. *J. Org. Chem.* **2007**, *72*, 1634.
(29) Bertelson, R. C. In *Photochromism*; Brown, G. H., Ed.; Wiley: New York, 1971, Chapter 10 and references therein.
(30) *Photochromism: Molecules and Systems*; Duerr, H., Bouas-Laurent, H., Eds.; Elsevier: Amsterdam, 1990.
(31) Crano, J. C.; Flood, T.; Knowles, D.; Kumar, A.; Gemert, B. V. *Pure Appl. Chem.* **1996**, *68*, 1395.
(32) *Organic Photochromic and Thermochromic Compounds*; Crano, J. C., Guglielmetti, R., Eds.; Plenum Press: New York, 1999; Vols. *1* and *2*.
(33) (a) Hepworth, J. D.; Heron, B. M. In *Progress in Heterocyclic Chemistry*; Gribble, G. W., Joule, J., Eds.; Elsevier Science: New York, 2005; Vol. *17*, p 33. (b) Minkin, V. I. *Chem. Rev.* **2004**, *104*, 2751.
(34) (a) Van Gemert, B.; Kumar, A.; Knowles, D. B. *Mol. Cryst. Liq. Cryst.* **1997**, *297*, 131. (b) Pozzo, J. L.; Lokshin, V.; Samat, A.; Guglielmetti, R.; Dubest, R.; Aubard, J. *J. Photochem. Photobiol. A.* **1998**, *114*, 185. and references therein. (c) Moustrou, C.; Rebière, N.; Samat, A.; Guglielmetti, R.; Yassar, A. E.; Dubest, R.; Aubard, J. *Helv. Chim. Acta* **1998**, *81*, 1293. (d) Martins, C. I.; Coelho, P. J.; Carvalho, L. M.; Oliveira-Campos, A. M. F.; Samat, A.; Guglielmetti, R. *Helv. Chim. Acta* **2003**, *86*, 570. (e) Salvador, M. A.; Coelho, P. J.; Burrows, H. D.; Oliveira, M. M.; Carvalho, L. M. *Helv. Chim. Acta* **2004**, *87*, 1400. (f) Paramonov, S.; Delbaere, S.; Fedorova, O.; Fedorov, Y.; Lokshin, V.; Samat, A.; Vermeersch, G. *J. Photochem. Photobiol. A.* **2010**, *209*, 111. (g) Sousa, C. M.; Pina, J.; de Melo, J. S.; Berthet, J.; Delbaere, S.; Coelho, P. J. *Org. Lett.* **2011**, *13*, 4040.
(35) (a) Moorthy, J. N.; Venkatakrishnan, P.; Sengupta, S.; Baidya, M. *Org. Lett.* **2006**, *8*, 4891. (b) Moorthy, J. N.; Venkatakrishnan, P.; Samanta, S. *Org. Biomol. Chem.* **2007**, *5*, 1354. (c) Moorthy, J. N.; Venkatakrishnan, P.; Samanta, S.; Kumar, D. K. *Org. Lett.* **2007**, *9*, 919. (d) Moorthy, J. N.; Koner, A. L.; Samanta, S.; Roy, A.; Nau, W. M. *Chem.—Eur. J.* **2009**, *15*, 4289. (e) Moorthy, J. N.; Mandal, S.; Parida, K. N.; Samanta, S. *J. Org. Chem.* **2011**, *76*, 7406. (f) Moorthy, J. N.; Mandal, S.; Parida, K. N. *Org. Lett.* **2012**, *14*, 2438.
(36) Janke, R. H.; Haufe, G.; Wuerthwein, E.-U.; Borkent, J. H. *J. Am. Chem. Soc.* **1996**, *118*, 6031.
(37) Delbaere, S.; Houze, B. L.; Bochu, C.; Teral, Y.; Campredon, M.; Vermeersch, G. *J. Chem. Soc., Perkin Trans. 2* **1998**, 1153.
(38) Kodama, Y.; Nakabayashi, T.; Segawa, K.; Hattori, E.; Sakuragi, M.; Nishi, N.; Sakuragi, H. *J. Phys. Chem. A* **2000**, *104*, 11478.
(39) Hobley, J.; Malatesta, V.; Hatanaka, K.; Kajimoto, S.; Williams, S. L.; Fukumura, H. *Phys. Chem. Chem. Phys.* **2002**, *4*, 180.
(40) Moine, B.; Buntinx, G.; Poizat, O.; Rehault, J.; Moustrou, C.; Samat, A. *J. Phys. Org. Chem.* **2007**, *20*, 936.
(41) During our investigations, Frigoli et al. reported photochromism of napthothopyran derivatives in which intramolecular C-H$\cdots\pi$ bonds have been shown to stabilize TC isomer of the *o*-quinonoid intermediate, see: Frigoli, M.; Maurel, F.; Delbaere, S.; Marrot, J.; Oliveira, M. M. *Org. Lett.* **2012**, *14*, 4150.
(42) Martins, C. I.; Coelho, P. J.; Carvalho, L. M.; Oliveira-Campos, A. M. F. *Tetrahedron Lett.* **2002**, *43*, 2203.
(43) Gabbutt, C. D.; Hepworth, J. D.; Heron, B. M.; Thomas, D. A.; Kilner, C.; Partington, S. M. *Heterocycles* **2004**, *63*, 567.
(44) Song, L.; Yang, Y.; Zhang, Q.; Tian, H.; Zhu, W. *J. Phys. Chem. B* **2011**, *115*, 14648.
(45) (a) Goedicke, C.; Stegemeyer, H. *Tetrahedron Lett.* **1970**, *11*, 937. (b) Martin, R. H.; Marchant, M. J. *Tetrahedron Lett.* **1972**, *13*, 3707. (c) Borkent, J. H.; Laarhoven, W. H. *Tetrahedron* **1978**, *34*, 2565.
(46) (a) Martin, R. H.; Marchant, M. J. *Tetrahedron* **1974**, *30*, 347. (b) Scheruebl, H.; Fritzsche, U.; Mannschreck, A. *Chem. Ber.* **1984**, *117*, 336.
(47) *Molecular Devices and Machines*; Balzani, V., Venturi, M., Credi, A., Eds.; Wiley-VCH: Weinheim, 2003.
(48) Bazan, G. C. *J. Org. Chem.* **2007**, *72*, 8615.
(49) Tour, J. M. *J. Org. Chem.* **2007**, *72*, 7477.
(50) Benight, S. J.; Knorr, D. B., Jr.; Johnson, L. E.; Sullivan, P. A.; Lao, D.; Sun, J.; Kocherlakota, L. S.; Elangovan, A.; Robinson, B. H.; Overney, R. M.; Dalton, L. R. *Adv. Mater.* **2012**, *24*, 3263.
(51) de Silva, A. P.; Vance, T. P.; Wannalerse, B.; West, M. E. S. In *Molecular Switches*; Feringa, B. L., Browne, W. R., Eds.; Wiley-VCH: Weinheim, 2011; Vol. *2*.
(52) *Mathematical Logic for Computer Science*; Ben-Ari, M., Ed.; Prentice-Hall: Hemel Hempstead, 1993.
(53) de Silva, A. P.; McClenaghan, N. D. *Chem.—Eur. J.* **2004**, *10*, 574.
(54) Gunnlaugsson, T.; MacDónail, D. A.; Parker, D. *Chem. Commun.* **2000**, 93.
(55) Gust, D.; Andréasson, J. Y.; Pischel, U.; Moore, T. A.; Moore, A. L. *Chem. Commun.* **2012**, *48*, 1947.
(56) Konry, T.; Walt, D. R. *J. Am. Chem. Soc.* **2009**, *131*, 13232.
(57) Berkovic, G.; Krongauz, V.; Weiss, V. *Chem. Rev.* **2000**, *100*, 1741.
(58) Irie, M. *Chem. Rev.* **2000**, *100*, 1685.
(59) Minkin, V. I. In *Molecular Switches*; Feringa, B. L., Browne, W. R., Wiley-VCH: Weinheim, 2011; Vol. *1*.
(60) Hirshberg, Y. *J. Am. Chem. Soc.* **1956**, *78*, 2304.
(61) Yokoyama, Y. *Chem. Rev.* **2000**, *100*, 1717.

(62) Guo, X.; Zhou, Y.; Zhang, D.; Yin, B.; Liu, Z.; Liu, C.; Lu, Z.; Huang, Y.; Zhu, D. *J. Org. Chem.* **2004**, *69*, 8924.
(63) Oliveira, M. M.; Salvador, M. A.; Delbaere, S.; Berthet, J.; Vermeersch, G.; Micheau, J. C.; Coelho, P. J.; Carvalho, L. M. *J. Photochem. Photobiol. A* **2008**, *198*, 242.
(64) Norsten, T. B.; Peters, A.; McDonald, R.; Wang, M.; Branda, N. R. *J. Am. Chem. Soc.* **2001**, *123*, 7447.
(65) Heller, H. G.; Hughes, D. S.; Hursthouse, M. B.; Rowles, N. G. *Chem. Commun.* **2000**, 1397.